Ann Nucl Med (2014) 28:571–579
DOI 10.1007/s12149-014-0850-9

ORIGINAL ARTICLE

Higher reliability of 18F-FDG target background ratio compared to standardized uptake value in vulnerable carotid plaque detection: a pilot study

Artor Niccoli Asabella · Marco M. Ciccone · Francesca Cortese · Pietro Scicchitano · Michele Gesualdo · Annapaola Zito · Alessandra Di Palo · Domenico Angiletta · Guido Regina · Andrea Marzullo · Giuseppe Rubini

Received: 27 December 2013 / Accepted: 1 April 2014 / Published online: 16 April 2014

Abstract
Objective To evaluate the role of [18F]-fluorodeoxyglucose positron emission tomography/computer tomography [18F-FDG PET/CT] comparing target background ratio (TBR) and standardized uptake value (SUV) with the histopathological inflammatory status of the carotid plaques.
Background Vulnerable carotid plaques are the primary cause of acute cerebrovascular events. 18F-FDG PET/CT represents a morpho-functional technique able to identify the highly inflamed and most vulnerable carotid plaques. Several literature studies experimented this new method to identify vascular inflammation, but few have effectively compared PET/CT results with plaque histological data and no studies had directly compared TBR to SUV.
Methods Thirty-two consecutive patients (20 men and 12 women, mean age 74 ± 8 years) undergoing carotid endarterectomy were enrolled and studied with carotid 18F-FDG PET/CT. Maximum and mean SUV and TBR were used to quantify 18F-FDG uptake while surgical specimens were analyzed by optical microscopy to identify inflamed carotid plaques, with evaluation of macrophages infiltration by mean of immunohistochemistry. On the basis of the presence of inflammation at the histological analysis, we divided population in two groups: group A ($n = 12$) patients with inflamed carotid plaques and group B ($n = 20$) patients with non-inflamed ones, then crossed and evaluated the histological data with 18F-FDG PET/CT findings.
Results SUV max and SUV mean values resulted higher in group A (respectively, 2.14 ± 0.77 and 1.99 ± 0.68) than in group B (respectively, 1.79 ± 0.37 and 1.64 ± 0.34) without reaching a statistical significance (p = ns). TBR max and TBR mean values resulted higher in group A (respectively, 1.42 ± 0.32 and 1.34 ± 0.26) than in group B (respectively, 1.16 ± 0.19 and 1.03 ± 0.20) with a statistically significant differences between the two groups and carotid inflammation (respectively, $p < 0.01$ and $p < 0.001$).
Conclusion TBR (max and mean values) is a more reliable parameter than SUV in identifying inflamed plaques. Although limited by the small population analyzed, our results suggest the important role of 18F-FDG PET/CT, using TBR, in identification of high-risk carotid atherosclerotic plaques.

Keywords PET/CT · Vulnerable carotid plaques · Histology

A. Niccoli Asabella (✉) · A. Di Palo · G. Rubini
Nuclear Medicine Unit, D.I.M., University of Bari "Aldo Moro", Piazza G. Cesare 11, 70124 Bari, Italy
e-mail: artor.niccoliasabella@uniba.it

M. M. Ciccone · F. Cortese · P. Scicchitano · M. Gesualdo · A. Zito
Cardiovascular Diseases Section, D.E.T.O., University of Bari "Aldo Moro", Bari, Italy

D. Angiletta · G. Regina
Vascular Surgery Unit, D.E.T.O., University of Bari "Aldo Moro", Bari, Italy

A. Marzullo
Pathological Anatomy Unit, D.E.T.O., University of Bari "Aldo Moro", Bari, Italy

Introduction

Atherosclerotic process represents nowadays the main cause of cerebrovascular disease in western countries, thus the most important determinant of morbidity and mortality over there [1]. In particular, complicated carotid plaques

are currently considered the primary cause of acute cerebrovascular events [2].

Adverse clinical events related to carotid atherosclerosis are largely due to plaque instability, which is able to induce plaque rupture and thrombi and emboli generation [3]. The correct diagnostic evaluation of vulnerable carotid plaques is therefore of primary importance for a prompt diagnosis, prevention, and treatment of cerebrovascular events. Surgical removal of unstable plaques represents the final intervention capable of reducing the incidence of fatal events [4]. Imaging techniques can identify plaque treatment-related changes, and therefore could be used as a marker of therapeutic efficacy [5].

Traditional methods exploring carotid luminal stenosis (echo color Doppler, magnetic resonance imaging, computer tomography, and angiography) are not able to reliably identify the unstable plaques. In fact, the degree of stenosis does not represent the only factor predictive of events: unstable non-stenotic plaques can rupture, while stable stenotic ones can lay dormant for years [6].

Positron emission tomography/computer tomography with the use of 18F-fluorodeoxyglucose, [18F-FDG PET/CT], represents an emerging morpho-functional technique able to identify the highly inflamed and consequently the most vulnerable carotid plaques [7, 8]. Several studies demonstrated that 18F-FDG uptake reflects inflammatory activation of plaque macrophages and potentially the plaque vulnerability [5, 9]. Macrophage infiltrate plays, in fact, an essential role in plaque rupture, as it is associated with an increased expression of scavenger receptors. The receptors bind and internalize modified low-density lipoprotein determining foam cells formation, able to release several proteases and cytokines, which lead to plaque rupture [10]. Several literature studies experimented this new method to identify vascular inflammation, but few have effectively compared PET/CT results with plaque histological data [7, 8, 11]. Up to date, no studies of direct comparison between Standardized Uptake Value (SUV), Target Background Ratio (TBR), and the plaque histological data are reported.

The aim of our study was to evaluate the role of [18F]-fluorodeoxyglucose positron emission tomography/computer tomography [18F-FDG PET/CT] comparing TBR and SUV with the histopathological inflammatory status of the carotid plaques.

Materials and methods

Thirty-two consecutive patients, admitted to the Department of Vascular Surgery, were investigated. All the patients had indication to carotid endarterectomy as they had an ultrasound diagnosis of significant carotid artery stenosis (>70 %) or non-significant stenosis complicated by cerebral ischemic disorders according to the current guidelines [12]. Before surgery (range 1–10 days; mean 4.4), they underwent 18F-FDG PET/CT of head, neck and thorax; moreover, patients underwent carotid ultrasound to detect carotid intima media thickness (C-IMT) and to classify carotid atherosclerotic plaques according to echogenicity.

Plaques removed during surgery were subsequently analyzed by an expert pathologist to detect in particular the presence of inflammation. Data obtained were then compared with 18F-FDG PET/CT results. According to the literature and the reports from the pathologist, we identified two groups: group A (12 patients) composed by patients showing inflamed carotid plaques, and group B (20 patients) formed by subjects with non-inflamed carotid ones [9, 11]. We directly compared 18F-FDG PET/CT data with those obtained from the histological analysis of plaques.

The study was approved by the local ethic committee and carried out in accordance with the principles of the Helsinki Declaration; all patients gave informed consent before entering the study.

Clinical evaluation

Major characteristics, clinical status and cardiovascular risk factor of 32 examined patients, are summarized in Table 1. Study population included 20 men (63 %) and 12 women (37 %), their age [mean ± standard deviation (SD)] was 74 ± 8 years (range 56–85).

Cardiovascular risk factors were distributed as follows: a total of 27 (84 %) patients suffered from arterial

Table 1 Demographic and clinical characteristics of study population

	Patients ($n = 32$)
Men/women *n* (%)	20 (63)/12 (37)
Age (years)[a]	74 ± 8
Range of age (years)	56–85
Weight (kg)[a]	73 ± 12
Height (m)[a]	1.64 ± 0.08
BMI (kg/m^2)[a]	27 ± 4
Waist (cm)[a]	96 ± 11
Obese subjects *n* (%)	6 (19)
Overweight subjects *n* (%)	10 (31)
Smoking *n* (%)	17 (53)
Arterial Hypertension *n* (%)	27 (84)
Diabetes *n* (%)	13 (41)
Dyslipidemia *n* (%)	27 (84)
Positive family history of CAD *n* (%)	3 (9)

n (%) numbers (percentage), *BMI* body mass index

[a] Mean ± standard deviation

hypertension, defined as systo/diastolic blood pressure values ≥140/90 mmHg or use of anti-hypertensive medication [13], 27 (84 %) from dyslipidemia, as they had total cholesterol ≥200 mg/dl or low-density lipoprotein cholesterol ≥130 mg/dl or high density lipoprotein cholesterol <45 mg/dl or triglycerides ≥150 mg/dl or they used lipid-lowering agents [14], 13 (41 %) were diabetic, because they had fasting glucose level ≥126 mg/dl, a self-reported physician diagnosis or were under pharmacologic treatment [15], 6 (19 %) were obese while 10 (31 %) overweight, as they had a body mass index ≥30 kg/m^2 and ranging from 25 and 30 kg/m^2, respectively, [16] and finally, we considered "current daily smoker" subjects with a regular smoke abuse of at least 5 cigarettes/day during the previous 3 months or which had stopped smoking <1 year before his/her admittance to the our department, a total of 17 (53 %) in our sample. Moreover, 3 (9 %) patients referred to have a positive family history of coronary artery disease that is one or more first-degree relatives with cardiac ischemic disease at any age [17].

All patients were in optimal pharmacological treatment before enrolment. Due to their clinical conditions and morphological vessels alterations, all of them were on statin and aspirin therapy. Anti-hypertensive treatment at maximum doses borne by the patients was based on antagonism of renin-angiotensin-aldosterone system.

Carotid ultrasound evaluation

The evaluations were performed with patients in supine position, with the neck extended and the head turned contralaterally by about 45°. The C-IMT was defined as the distance between the lumen-intima and media–adventitia borders of the vessel, ultrasonographically identified by a double hypoechoic line, and calculated using scans of the lengthwise axis, according to the method described by Pignoli et al. [18, 19] C-IMT value was obtained as the arithmetical mean of the values calculated in the following three zones: proximally, about 2 cm above the flow-divider, distally about 1/2 cm above the flow-divider and in the middle zone. Moreover, we classified plaques according to echogenicity in hyperechoic, isoechoic, hypoechoic, and mixed plaques. Plaque echogenicity was compared with blood and adjacent adventitia as follows: low echoes were defined as those strictly close to that of blood, and medium to high echoes were those similar to or greater than adventitia [20].

Histological and immunohistochemical assessment of carotid plaque

Carotid endarterectomy was performed under local anesthesia by the same team of vascular surgeons using a standardized protocol [21]. Endarterectomy specimens were removed and fixed in 10 % neutral formalin for 24–48 h. Serial cross sections were then obtained, at intervals of about 3 mm, to have representative patterns of the whole sample.

Specimens were paraffin embedded, and then cut in section of 4 micron thick, and, if too hard to cut, previously submitted to a decalcification procedure to avoid rupture; then, they were subsequently stained with hematoxylin-eosin, Masson trichromic and van Gieson stains, the latter specific for elastic fibers, assessing, in a blinded manner by optical microscopy, the presence and the degree of inflammation.

Moreover, sections were incubated with anti-CD68 monoclonal antibody (clone PGM1, Dako—Glostrup, Denmark) at a 1:100 dilution after antigen unmasking (EDTA buffer in DAKO PTlink) to identify and quantify the presence of macrophages. Immunohistochemistry was performed using the Dako "EnVision+" biotin-free enhanced labeled polymer method. Appropriate positive and negative controls were used.

Immunohistochemical staining

CD68 staining was analyzed and categorized in a blinded manner. Because of the inhomogeneous distribution of histochemical patterns, we applied the high reproducible semiquantitative analyses to describe the predominant histochemical characteristics of the entire sample [22].

Immunochemical setting was evaluated using a four level arbitrary score as follows: (−) absence of immune-positivity; (+) presence of sporadic CD68-positive cellular elements, mostly isolated; (++) presence of CD68-positive cellular elements arranged in small heaps; (+++) presence of CD68-positive cellular elements scattered in the plaque and organized into big piles (Fig. 1a, b). Plaques were considered inflamed if ranged (++) or (+++).

18F-FDG PET/CT imaging

18F-FDG PET/CT images were acquired with combined modality PET/CT (GE Discovery LSA, Waukesha, Wisconin, USA) that integrates a PET scanner (Advance nxI) to a 16-slice CT (Light Speed Plus). Prior to administration of fluorine-18-deoxyglucose (18F-FDG), all patients fasted for at least 8 h and the measurement of capillary blood glucose (<160 mg/ml) were performed. To avoid artefacts caused by the muscle's physiological uptake, they were instructed to limit any physical activity after radiopharmaceutical administration and before the examination. The image acquisition was obtained 50 min after the intravenous injection of 37 MBq/10 kg of 18F-FDG. During this

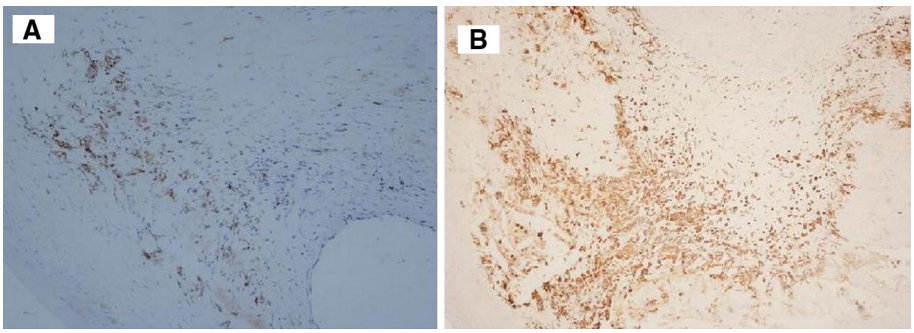

Fig. 1 **a** Sparse macrophages CD 68 positive in the atherosclerotic plaque (CD 68 immunostaining; magnification ×100), score ++. **b** Diffuse presence of CD 68 positive macrophages in the plaque shoulder (CD 68 immunostaining; magnification ×40), score +++

time, patients were hydrated by drinking 500 ml of water and urinate as needed. Muscle relaxant drugs were not administered. 18F-FDG PET/CT scan was carried out by the vertix of the head to the diaphragm. Patients were instructed to breathe quietly during the examination. The CT acquisition parameters were: 89 mA (auto), 120 kV, slice thickness 3.75 mm, tube rotation time 0.8 ms, collimation field of view (FOV) of 50 cm. The CT images were reconstructed with a filtered back-projection. The CT data were used for attenuation correction of PET scanning, which was performed immediately after the acquisition of CT images. The CT scans were obtained without administration of contrast enhancer. The PET acquisition was obtained in caudal-cranial direction, acquisition technique with 3D interactive reconstruction.

Image analysis

A nuclear physician evaluated 18F-FDG PET/CT of the selected patient at a dedicated Advantage 4.3 Workstation (GE Healthcare, Waukesha, Wisconsing, USA). The images of 18F-FDG PET/CT were displayed in three orthogonal planes as PET images, CT and fusion images. The 18F-FDG PET/CT evaluated the atherosclerotic carotid plaque and the superior cava vein. The scans were analyzed visually and semi-quantitatively. Arterial 18F-FDG uptake in the neck was measured by drawing a region of interest (ROI) around the carotid artery on every slice of the co-registered transaxial PET/CT images. 18F-FDG uptake was measured along the length of the carotid plaque, subsequently removed during endarterectomy, starting at the bifurcation and extending inferiorly and superiorly every 4 mm.

On each image slice, SUV max of 18F-FDG in the ROI was calculated as the maximum pixel activity. The SUV was automatically calculated by the workstation software as the ratio between the accumulation of 18F-FDG (MBq/ml) in an area of interest (drawn on the images corrected for attenuation) and the activity

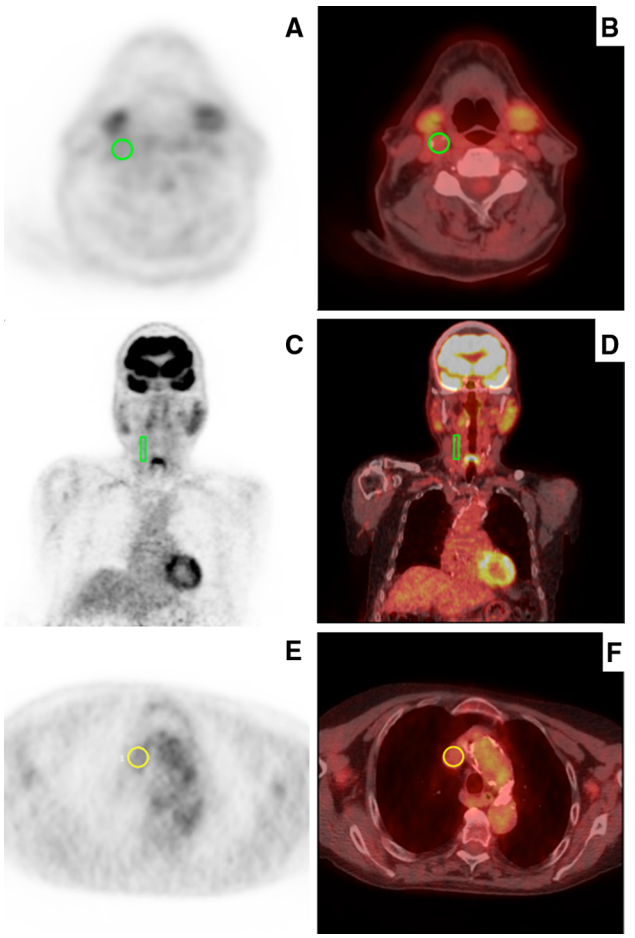

Fig. 2 18F-FDG PET/CT images: **a** Positron emission tomography (PET) image of a transverse section with the region of interest (*green*) around the carotid plaques to analyse; **b** fusion CT/PET image of a transverse section with the region of interest (*green*) around the carotid plaques; **c** Positron emission tomography (PET) image of a coronal section with the region of interest (*green*) around the carotid plaques; **d** fusion CT/PET image of a coronal section with the region of interest (*green*) around the carotid plaques; **e** Positron emission tomography (PET) image of a transverse section with the region of interest (*yellow*) around the superior cava vein; **f** fusion CT/PET image of a transverse section with the region of interest (*yellow*) around the superior cava vein

Table 2 Ultrasound, PET/CT and histopathological characteristics of carotid plaques of whole study population

Ultrasound findings		PET/CT findings	Mean ± SD	Range	Histological analysis	
RCA *n* (%)	13 (41)	SUV max	1.98 ± 0.64	1.2–4.2	Inflammation *n* (%)	12 (37.5)
LCA *n* (%)	19 (59)	SUV mean	1.77 ± 0.51	0.9–3.5	No inflammation *n* (%)	20 (62.5)
Hyperechoic plaques *n* (%)	7 (22)	TBR max	1.26 ± 0.27	0.82–1.93	CD 68 data	
Isoechoic plaques *n* (%)	4 (12)	TBR mean	1.13 ± 0.26	0.76–1.79	CD 68 (+++) *n* (%)	8 (25)
Hypoechoic plaques *n* (%)	9 (28)				CD 68 (++) *n* (%)	4 (12.5)
Mixed plaques *n* (%)	12 (38)				CD 68 (+) *n* (%)	3 (9.4)
Grade of stenosis %	77 ± 12				CD 68 (−) *n* (%)	17 (53.1)
R C-IMT (mm)	0.64 ± 0.19					
L C-IMT (mm)	0.98 ± 0.2					

n (%) numbers (percentage), *PET* positron emission tomography, *CT* computer tomography, *CA* internal carotid artery, *R* right, *L* left, *C-IMT* carotid intima media thickness, *SUV* standardized uptake value, *TBR* target background ratio

administered (MBq), for the weight (kg) according to the following formula:

SUV = ROI activity (MBq/ml)/[injected dose (MBq)/body weight (kg)].

To obtain a background value for 18F-FDG uptake, SUV max and mean were measured in a venous structure. To accomplish this, an ROI was placed within the center of a large vein (superior cava vein) in an area devoid of significant activity. We calculated the TBR max as the SUV max normalized to venous SUV max and TBR mean as the SUV mean normalized to venous SUV mean [5].

Sagittal and coronal image reconstruction was performed to ensure correct ROI placement (Fig. 2).

Statistical analysis

The data are given as mean values ± SD, and categorical variables as frequencies and percentage. Between-group comparisons were performed by t test for independent sample if the distribution resulted normal at Kolmogorov–Smirnov test and at Lilliefors test. As nonparametric methods, we used Mann–Whitney *U* test for two independent samples and Kruskal–Wallis ANOVA for multiple independent samples' comparison. Frequencies were compared using the Chi squared or Fisher's exact test. Analyses were made using STATISTICA 7 software (StatSoft Inc., Tulsa, Oklahoma, USA).

Results

Ultrasound, PET/CT, and histopathological characteristics of the carotid plaques of all patients are summarized in Table 2. Thirteen (41 %) plaques were localized in the right carotid artery, while 19 (59 %) in the left one, with a grade of stenosis of 77 ± 12 %. C-IMT value of the right carotid artery resulted 0.64 ± 0.19 mm, while the left one 0.98 ± 0.2 mm, moreover, as regard the echogenicity, we detected 7 (22 %) hyperechoic, 4 (12 %) isoechoic, 9 (28 %) hypoechoic and 12 (38 %) mixed plaques.

18F-FDG PET/CT semiquantitative evaluation of all study population highlighted SUV max and mean values, respectively, ranged 1.2–4.2, mean 1.98 ± 0.64 and ranged 0.9–3.5, mean 1.77 ± 0.51; TBR max and mean values were, respectively, ranged 0.82–1.93, mean 1.26 ± 0.27 and ranged 0.76–1.79, mean 1.13 ± 0.26.

The histological analysis identified 12 (37 %) inflamed plaques and 20 (63 %) non-inflamed ones. The results were perfectly consistent with those of immunohistochemical assessment. In fact, the 12 (37 %) inflamed plaques showed to have a large inflammatory component, (++) in 4 cases and (+++) in the other 8 cases composed by macrophages (CD 68 positive cells), distributed both in the vascular wall in contiguity of the plaque, both within the plaque itself, frequently organized in piles. The remaining 20 (63 %) non-inflamed ones, showed, on the contrary, absence of immunopositivity, (−) in 17 cases, or presence of sporadic positive CD 68 cellular elements mostly isolated, (+) in 3 cases.

The comparison between the two groups (A subjects with inflamed carotid plaques and B subjects with non-inflamed carotid ones) as regard demographic, clinical, anatomical, ultrasound and 18F-FDG PET/CT findings are reported in Table 3. The data showed no statistically significant differences between the two groups as regards demographic, clinical, anatomical and ultrasound findings.

In group A, SUV max and mean ranged, respectively, from 1.3 to 4.2 mean 2.14 ± 0.77 and from 1.2 to 3.5, mean 1.99 ± 0.68. In group B SUV max and mean ranged, respectively, from 1.2 to 2.5 mean 1.79 ± 0.37 and from 0.9 to 2.2 mean 1.64 ± 0.34 (Table 3). As regard TBR values, in group A, TBR max and mean ranged, respectively, from 0.82 to 1.93 mean 1.42 ± 0.32 and from 0.8 to 1.79 mean 1.34 ± 0.26. In group B TBR max and mean

Table 3 Comparison between general (demographic and clinical), anatomical, ultrasound, 18F-FDG PET/CT and histopathological characteristics of patients with inflamed carotid plaques (group A) vs. patients with non-inflamed ones (group B)

	Group A ($n = 12$)	Group B ($n = 20$)
General characteristics		
Men *n* (%)	7 (58)	13 (65)
Women *n* (%)	5 (42)	7 (35)
Age (years)[a]	73 ± 10	74 ± 7
Weight (kg)[a]	77 ± 11	68 ± 10
Height (m)[a]	1.63 ± 0.1	1.65 ± 0.1
BMI (kg/m^2)[a]	29 ± 3	25 ± 3
Waist (cm)[a]	100 ± 9	94 ± 9
Smoking *n* (%)	6 (50)	11 (55)
Arterial hypertension *n* (%)	11 (92)	16 (80)
Diabetes *n* (%)	6 (50)	7 (35)
Dyslipidemia *n* (%)	10 (83)	17 (85)
Ultrasound findings		
R-CA *n* (%)	5 (42 %)	8 (40 %)
L-CA *n* (%)	7 (58 %)	12 (60 %)
Grade of stenosis (%)[a]	75 ± 13	79 ± 12
Hyperechoic plaques *n* (%)	1 (8)	6 (30)
Isoechoic plaques *n* (%)	1 (8)	3 (15)
Hypoechoic plaques *n* (%)	5 (42)	4 (20)
Mixed plaques *n* (%)	5 (42)	7 (35)
R-CIMT (mm)[a]	0.92 ± 0.3	1.08 ± 0.3
L-CIMT (mm)[a]	1.02 ± 0.2	1.08 ± 0.2
PET/CT findings		
SUV max[a]	2.14 ± 0.77	1.79 ± 0.37
SUV max (range)	1.3–4.2	1.2–2.5
SUV mean[a]	1.99 ± 0.68	1.64 ± 0.34
SUV mean (range)	1.2–3.5	0.9–2.2
TBR max[a]	1.42 ± 0.32**	1.16 ± 0.19**
TBR max (range)	0.82–1.93	0.82–1.64
TBR mean[a]	1.34 ± 0.26***	1.03 ± 0.20***
TBR mean (range)	0.8–1.79	0.76–1.5

n (%) numbers (percentage), *CA* carotid artery, *CIMT* common carotid intima media thickness, *R* right, *L* left, *PET* positron emission tomography, *CT* computer tomography, *SUV* standardized uptake value, *TBR* target background ratio

** $p < 0.01$; *** $p < 0.001$

[a] Mean ± standard deviation

ranged, respectively, from 0.82 to 1.64 mean 1.16 ± 0.19 and from 0.76 to 1.5 mean 1.03 ± 0.20 (Table 3). SUV max, SUV mean, TBR max and TBR mean values resulted higher in group A respect to group B, demonstrating that both parameters are in agreement with the presence of carotid inflammation (Table 3; Fig. 3). Furthermore, the comparison of SUV max and mean between the two groups showed no significant differences while statistically significant differences were found as regard TBR max ($t = 2.89$, $p < 0.01$) and mean ($t = 3.7$, $p < 0.001$).

Discussion

In last decade, great attention has been focused on the research of imaging techniques capable of highlight vulnerable carotid plaques at high risk of complication and therefore of cerebrovascular events and death. A great interest has been focused on the research of non-invasive methods able to identify patients with carotid atherosclerotic plaques at risk of rupture, which would benefit from surgical removal. PET/CT method with the use of 18F-FDG represents an emerging and an innovative technique able to noninvasively detect the metabolically active carotid plaques at increased risk of rupture. 18F-FDG, in fact, accumulates in macrophages, considered causally related to plaques complications [23, 24].

Several animal and clinical studies tried to explain the mechanism of 18F-FDG uptake in atherosclerotic plaques. Some authors suggest that 18F-FDG uptake is correlated to macrophages density because glucose is essential substrate for energy production in various cells [9]. 18F-FDG uptake reflects inflammatory activation of plaque macrophages and potentially the tendency of plaque to rupture [5, 9]. Furthermore, it is reported that the use of statins decreases 18F-FDG uptake in patients with atherosclerosis [25], this is probably related to anti-inflammatory effect of statin's therapy.

In addition, Tawakol et al. [5, 23] demonstrated a correlation between the arterial uptake of 18F-FDG and macrophage presence, proposing 18F-FDG uptake as an indicative measure of arterial inflammation, while other authors showed a significantly higher uptake in vivo of 18F-FDG in symptomatic carotid plaques than in asymptomatic ones, suggesting that inflammation is present to a greater degree in symptomatic plaques [24].

Moreover, Chen et al. [26] showed a link between 18F-FDG uptake and cardiovascular events such as myocardial infarction and stroke. Recently, Figueroa et al. [11] highlighted that inflammation, detected by 18F-FDG uptake, is increased in plaques containing high-risk morphological features at the histological analysis, supporting the concept that the burden of morphological abnormalities of carotid plaques is correlated with the 18F-FDG uptake, considered a measure of plaque vulnerability. Other authors, Folco et al. [27], suggest that intraplaque hypoxia may contribute to the higher intensity of 18F-FDG accumulation in atheromata.

Although several studies have showed an association between plaque 18F-FDG uptake and inflammation, suggesting 18F-FDG PET/CT method as a promising tool for

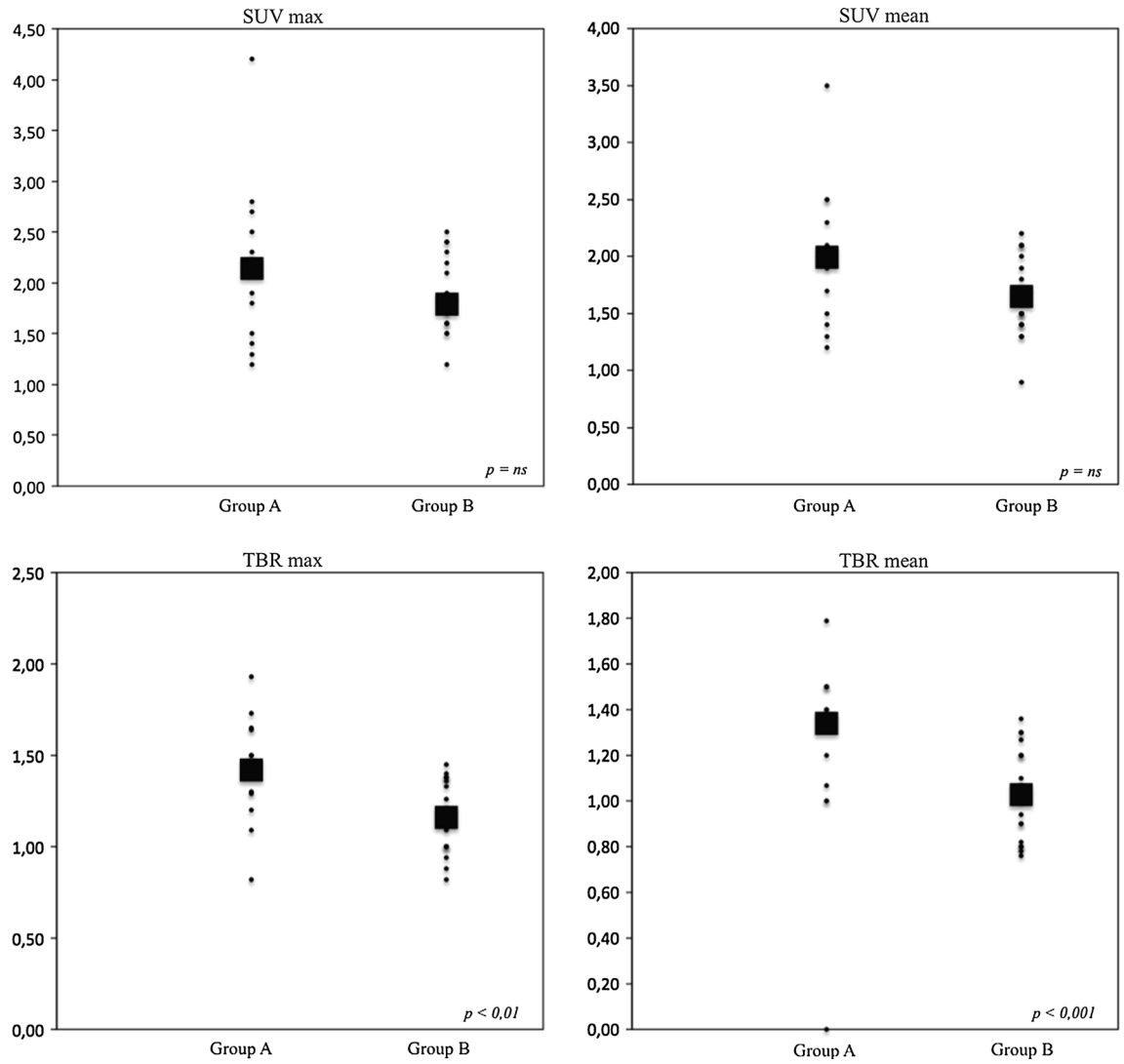

Fig. 3 Comparison of SUV and TBR values between the two groups; the *square* indicates the mean value. *Graphs* showed no significant differences as regard SUV max and mean values (p = ns) while statistically significant differences were found as regard TBR max (1.42 ± 0.32 in group A vs. 1.16 ± 0.19 in group B, $p < 0.01$) and mean (1.34 ± 0.26 in group A vs. 1.03 ± 0.20 in group B, $p < 0.001$)

detecting patients candidate to carotid endarterectomy [28, 29]. Our results, demonstrating the differences in TBR values found among the analyzed groups, significantly expand the validity of 18F-FDG PET/CT method.

In our study, we evaluated in vivo 18F-FDG uptake in carotid plaques subsequently analyzed histologically, demonstrating a significant agreement between 18F-FDG PET/CT results and histological analysis. Our results showed higher 18F-FDG uptake in presence of inflammatory infiltrate, in which we demonstrated with immunohistochemistry the presence of macrophages, cells always associated with carotid inflammation and then with carotid vulnerable plaques rupture [30].

Several studies have underlined that 18F-FDG uptake calculated by SUV or corrected for blood activity to produce the TBR are useful tools to evaluate plaque activity [5, 23, 24]. Rudd et al. [31] compared different methods of measurement of artery 18F-FDG uptake, demonstrating the reproducibility of the parameters SUV and TBR max and mean, but the choice of the better one is still debated.

Remarkably, we did not find any significant differences as regard SUV max and mean values between inflamed and non-inflamed plaques, but, by normalizing carotid SUV values for blood 18F-FDG activity (TBR max and mean values), we demonstrated a significant agreement with the presence of histological inflammation; both TBR max and TBR mean values resulted in fact significantly associated with the presence of carotid inflammation (Table 3).

Our data suggest that a methodological and rigorous evaluation of TBR max and mean is more reliable than SUV in the identification of high-risk plaques in particular in patients with high risk of cardiovascular events.

The explanation of the better performance of TBR over SUV must consider some statistical and metabolic factors. The statistical analysis evidences that in both groups, the standard deviation of SUV max and mean is significantly higher than that of the standard deviation of TBR max and mean, respectively, Group A 0.77 and 0.68 vs. 0.32 and 0.26 and Group B 0.37 and 0.34 vs. 0.19 and 0.20 (Fig. 3). The normalization of 18F-FDG uptake to the blood activity, considered in TBR, allows to correct the error from the blood glucose level or insulin level and others factors that may influence SUV. In fact, oncologic PET/CT studies have shown that 18F-FDG uptake is diminished during hyperglycemia [32–35]. This effect, however, has not been evaluated in vascular PET imaging, but our results suggest that blood glucose or insulin levels may influence negatively the SUV and highlight the TBR role.

Limitations

Vascular calcification may arise as a result of both active and passive mechanisms in the arterial wall during atherogenesis. In this study, CT images of PET/CT were used only for the anatomical landmark and we did not evaluate arterial calcification although it is strongly considered as an independent predictor for cardiovascular events; this can be maybe a limit of our study. Considering that inflammation and calcification rarely overlapped within arteries [36] and that 18F-FDG is not the ideal radiotracers to evaluate the calcification we think that this limitation does not affect the results of our study. Further, authors have suggested the use of 18F-sodium Fluoride as a measure of calcifying plaque that correlates with cardiovascular risk factors [37].

Our study population was relatively limited, but all the 32 patients underwent endoarterectomy and every carotid plaque was analyzed histologically with evaluation of macrophages infiltration by mean of immunohistochemistry.

Conclusion

In our comparative study, carotid 18F-FDG PET/CT seems to be a valid tool in the detection of inflamed plaques at risk of rupture.

Only TBR max and mean values were in agreement with the presence of inflammation histologically confirmed, while no differences were found as regard SUV max and mean values among inflamed and non-inflamed plaques.

TBR max and mean showed to be the most reliable parameter in the identification of vulnerable plaques. Although limited by the small population analyzed, results suggested the important role of 18F-FDG PET/CT, using TBR parameter, in the identification of carotid atherosclerotic plaques at high risk. Our results are promising but other studies are needed to make our results more consistent.

Conflicts of interest None declared.

References

1. Roger VL, Go AS, Lloyd-Jones DM, Benjamin EJ, Berry JD, Borden WB, et al. Executive summary: heart disease and stroke statistics—2012 update: a report from the American Heart Association. Circulation. 2012;125:188–97.
2. Sitzer M, Trostdorf F. The unstable carotid stenosis: definition and biological processes. Hamostaseologie. 2003;23:61–6.
3. Libby P. Inflammation in atherosclerosis. Nature. 2002;420:868–74.
4. Chaturvedi S, Bruno A, Feasby T, Holloway R, Benavente O, Cohen SN, et al. Carotid endarterectomy—an evidence-based review: report of the Therapeutics and Technology Assessment Subcommittee of the American Academy of Neurology. Neurology. 2005;65:794–801.
5. Tawakol A, Migrino RQ, Hoffmann U, Abbara S, Houser S, Gerwitz H, et al. Noninvasive in vivo measurement of vascular inflammation with F-18 fluorodeoxyglucose positron emission tomography. J Nucl Cardiol. 2005;12:294–301.
6. de Vries Wallis BM, van Dam GM, Tio RA, Hillebrands JL, Slart RH, Zeebregts CJ. Current imaging modalities to visualize vulnerability within the atherosclerotic carotid plaque. J Vasc Surg. 2008;48:1620–9.
7. Meerwaldt R, Slart RH, van Dam GM, Luijckx GJ, Tio RA, Zeebregts CJ. PET/SPECT imaging: from carotid vulnerability to brain viability. Eur J Radiol. 2010;74:104–9.
8. Tahara N, Kai H, Nakaura H, Mizoguchi M, Ishibashi M, Kaida H, et al. The prevalence of inflammation in carotid atherosclerosis: analysis with fluorodeoxyglucose-positron emission tomography. Eur Heart J. 2007;28:2243–8.
9. Ogawa M, Ishino S, Mukai T, Asano D, Teramoto N, Watabe H, et al. (18)F-FDG accumulation in atherosclerotic plaques: immunohistochemical and PET imaging study. J Nucl Med. 2004;45:1245–50.
10. Riou LM, Broisat A, Dimastromatteo J, Pons G, Fagret D, Ghezzi C. Pre-clinical and clinical evaluation of nuclear tracers for the molecular imaging of vulnerable atherosclerosis: an overview. Curr Med Chem. 2009;16:1499–511.
11. Figueroa AL, Subramanian SS, Cury RC, Truong QA, Gardecki JA, Tearney GJ, et al. Distribution of inflammation within carotid atherosclerotic plaques with high-risk morphological features: a comparison between positron emission tomography activity, plaque morphology, and histopathology. Circ Cardiovasc Imaging. 2012;5:69–77.
12. Eckstein HH. Evidence-based management of carotid stenosis: recommendations from international guidelines. J Cardiovasc Surg (Torino). 2012;53:S3–13.
13. Mancia G, De Backer G, Dominiczak A, Cifkova R, Fagard R, Germano G, et al. 2007 ESH-ESC Practice Guidelines for the Management of Arterial Hypertension: ESH-ESC Task Force on

the Management of Arterial Hypertension. J Hypertens. 2007;25:1751–62.
14. American Diabetes Association. Diagnosis and classification of diabetes mellitus. Diabetes Care. 2010;33:S62–9.
15. National Cholesterol Education Program (NCEP) Expert Panel on Detection, Evaluation, and Treatment of High Blood Cholesterol in Adults (Adult Treatment Panel III). Third Report of the National Cholesterol Education Program (NCEP) Expert Panel on Detection, Evaluation, and Treatment of High Blood Cholesterol in Adults (Adult Treatment Panel III) Final Report. Circulation. 2002;106:3143–421.
16. Martínez JA, Kearney JM, Kafatos A, Paquet S, Martínez-González MA. Variables independently associated with self-reported obesity in the European Union. Public Health Nutr. 1999; 2:125–33.
17. Silberberg JS, Wlodarczyk J, Fryer J, Robertson R, Hensley MJ. Risk associated with various definitions of family history of coronary heart disease. The Newcastle Family History Study II. Am J Epidemiol. 1998;147:1133–9.
18. Touboul PJ, Hennerici MG, Meairs S, Adams H, Amarenco P, Bornstein N, et al. Mannheim carotid intima-media thickness consensus (2004–2006). Cerebrovasc Dis. 2007;23:75–80.
19. Pignoli P, Tremoli E, Poli A, Oreste P, Paoletti R. Intimal plus medial thickness of the arterial wall: a direct measurement with ultrasound imaging. Circulation. 1986;74:1399–406.
20. Arnold JA, Modaresi KB, Thomas N, Taylor PR, Padayachee TS. Carotid plaque characterization by duplex scanning: observer error may undermine current clinical trials. Stroke. 1999;30:61–5.
21. Kim TY, Choi JB, Kim KH, Kim MH, Shin BS, Park HK. Routine shunting is safe and reliable for cerebral perfusion during carotid endarterectomy in symptomatic carotid stenosis. Korean J Thorac Cardiovasc Surg. 2012;45:95–100.
22. Hellings WE, Pasterkamp G, Vollebregt A, Seldenrijk CA, De Vries JP, Velema E, et al. Intraobserver and interobserver variability and spatial differences in histologic examination of carotid endarterectomy specimens. J Vasc Surg. 2007;46:1147–54.
23. Tawakol A, Migrino RQ, Bashian GG, Bedri S, Vermylen D, Cury RC, et al. In vivo 18F-fluorodeoxyglucose positron emission tomography imaging provides a noninvasive measure of carotid plaque inflammation in patients. J Am Coll Cardiol. 2006;48:1818–24.
24. Rudd JH, Warburton EA, Fryer TD, Jones HA, Clark JC, Antoun N, et al. Imaging atherosclerotic plaque inflammation with [18F]-fluorodeoxyglucose positron emission tomography. Circulation. 2002;105:2708–11.
25. Tahara N, Kai H, Ishibashi M, Nakaura H, Kaida H, Baba K, et al. Simvastatin attenuates plaque inflammation: evaluation by fluorodeoxyglucose positron emission tomography. J Am Coll Cardiol. 2006;48:1825–31.
26. Chen W, Dilsizian V. (18)F-fluorodeoxyglucose PET imaging of coronary atherosclerosis and plaque inflammation. Curr Cardiol Rep. 2010;12:179–84.
27. Folco EJ, Sheikine Y, Rocha VZ, Christen T, Shvartz E, Sukhova GK, et al. Hypoxia but not inflammation augments glucose uptake in human macrophages. J Am Coll Cardiol. 2011;58: 603–14.
28. Sheikine Y, Akram K. FDG-PET imaging of atherosclerosis: Do we know what we see? Atherosclerosis. 2010;211:371–80.
29. Graebe M, Pedersen SF, Højgaard L, Kjaer A, Sillesen H. 18FDG PET and ultrasound echolucency in carotid artery plaques. JACC Cardiovasc Imaging. 2010;3:289–95.
30. Martinet W, Schrijvers DM, De Meyer GR. Molecular and cellular mechanisms of macrophage survival in atherosclerosis. Basic Res Cardiol. 2012;107:297.
31. Rudd JH, Myers KS, Bansilal S, Machac J, Pinto CA, Tong C, et al. Atherosclerosis inflammation imaging with 18F-FDG PET: carotid, iliac, and femoral uptake reproducibility, quantification, methods, and recommendations. J Nucl Med. 2008;49:871–8.
32. Shepherd PR, Kahn BB. Glucose transporters and insulin action implications for insulin resistance and diabetes mellitus. N Engl J Med. 1999;341:248–57.
33. Wahl RL, Henry CA, Ethier SP. Serum glucose: effects on tumor and normal tissue accumulation of 2-[F-18]-fluoro-2-deoxy-D-glucose in rodents with mammary carcinoma. Radiology. 1992;183:643–7.
34. Deichen JT, Prante O, Gack M, Schmiedehause K, Kuwert T. Uptake of [(18)F]fluorodeoxyglucose in human monocyte-macrophages in vitro. Eur J Nucl Med Mol Imaging. 2003;30:267–73.
35. Niccoli Asabella A, Iuele FI, Merenda N, Pisani AR, Notaristefano A, Rubini G. 18F-FDG PET/CT diabetes and hyperglycaemia. Nucl Med Rev Cent East Eur. 2013;16(2):57–61.
36. Rudd JH, Myers KS, Bansilal S, Machac J, Woodward M, Fuster V, et al. Relationships among regional arterial inflammation, calcification, risk factors, and biomarkers a prospective fluorodeoxyglucose positron-emission tomography/computed tomography imaging study. Circ Cardiovasc Imaging. 2009;2:107–15.
37. Derlin T, Wisotzki C, Richter U, Apostolova I, Bannas P, Weber C, et al. In vivo imaging of mineral deposition in carotid plaque using 18F-sodium fluoride. J Nucl Med. 2011;52:362–8.